International Journal of Engineering Research & Technology (IJERT)
ISSN: 2278-0181
Vol. 3 Issue 1, January - 2014

Influence of Reinforcement Ratio and Arrangement on Penetration Resistance of Concrete Panels Reinforced with Wire Steel Meshes : Numerical Simulation

Amin. M. S.* and Taha. A. K.**

*Lecturer Structural Engineering, Dept. of Civil Eng., M.T.C., Cairo
** M.Sc. Student, Dept. of Civil Eng. M.T.C., Cairo

Abstract

Different from plain concrete in which the strength mainly dominates its ability of resisting penetration, reinforced concrete may be influenced by both the concrete strength and the reinforcement ratio and arrangement. Reinforced concrete protective layers of fortified structures are considered key points in resisting missiles penetration. The usage of wire steel meshes reinforcement provides isotropic properties in two directions, high tensile strength, and high modulus of rupture. It also results in larger bond forces and reduces crack spacing and width compared to conventional reinforcement bars. Accordingly, A Nonlinear three-dimensional numerical simulation was carried out using AUTODYN 3D software, which use the hydrocodes to model projectile – targeted structure interaction problems. Fourteen numerical simulation tests were carried out on concrete panels (550 x 550 x 300 mm) that are reinforced with expanded wire steel meshes and subjected to 23 mm diameter steel ogive-nose projectile perpendicularly fired with striking velocity = 990 m/s. The parametric study aimed to study the influence of reinforcement ratio and arrangement on panel's penetration resistance. The parameters included are the reinforcement ratio; reinforcement position (rear face / front face); and reinforcement distribution along the panels thickness.
The results proved that using the wired steel meshes decreases the size of damage regions in the front and rear face of the panels. Increasing the reinforcement ratio has insignificant impact on the penetration resistance while the position and the distribution pattern of reinforcement proved to relatively influence the penetration resistance.

Keywords

Concrete Panels; Ferrocement; Penetration Resistance; Hydrocodes; Steel Projectile.

1. Introduction

The behaviour of concrete differs in dynamic loading compared to static loading. When a projectile hits concrete target, the concrete will crush and crack. The pressure at the front of the nose of the projectile is several times higher than the static uniaxial strength of concrete with an increase in the lateral pressure. Under the nose of the missile, concrete is exposed to confining pressure and behaves plastically, dissipating a large amount of energy. Since concrete is very weak in tension, the tensile wave obtained when the compressive wave hits the backside of the wall may cause scabbing at the backside, and cracking in the lateral direction [1].

Several researchers conducted experimental researches aiming to develop empirical formula that can predict the penetration depth in concrete panels caused by high speed ogive-nose projectile. An analytic/empirical study was carried out to develop an empirical model that predicts the penetration depth of multiple impacts into concrete targets. Using the multiple impact penetration and crater formation data, a single impact penetration model was extended to account for the degradation of the target strength with each subsequent impact [2&3]. The ballistic penetration experiments, conducted on concrete target – fragment steel projectile, show the linear dependence of the penetration depth on the striking velocity of the projectile. For the impact velocities between 300 and 1400 m/s post-test observation of the targets showed that the fragment penetration leads to the crater formation [4].

The penetration/perforation process of reinforced concrete includes initial cratering, tunnelling and rear cratering (shear plugging). Different from plain concrete in which the strength mainly dominates its ability of resisting penetration, reinforced concrete may be influenced by both the concrete strength and the amount of reinforcement. Penetration tests were carried out on regular strength concrete (RSC) and on high strength concrete (HSC) panels with different

reinforcement types [5, 6 &7]. The results showed that as the concrete strength increased from normal-strength to high-strength, energy absorption capacity and critical velocity of perforation increased. Different types of reinforcement and careful detailing can enhance the barrier's performance under impact, mainly by limiting the damaged area. It also, show that the concrete panels with closely spaced but small diameter wires, that had a relatively low reinforcement ratio, were less efficient against penetration or front face spalling, yet, relative to their low reinforcement ratio, they showed an enhanced resistance against perforation and scabbing.

Ferrocement is a highly versatile form of concrete reinforced with wire mesh [8], as mesh-reinforcing systems is used as layers of continuous expanded steel wire mesh. This form of reinforcement enables reinforcing in two directions; therefore, it has homogenous-isotropic properties in two directions and high reinforcement ratio. The average crack spacing decreases with increasing specific surface for both tension and flexure. However, other factors, such as the geometry of the reinforcement, also influence crack development. The average crack spacing corresponds closely to the transverse wire spacing, and the average crack width reduces as this spacing decreases. It is also able to absorb a large amount of energy during fracture under dynamic loading. This is thought to be due to the substantial energy requirement to de-bond and pull out or yield and fracture the expanded wire steel mesh as the cracks open at high loading rates. The improvements in impact resistance with the inclusion of expanded steel mesh vary widely and depend to a large extent on the energy and velocity of the impacting mass, the size of specimen and rigidity of supports, the type of test, and even the definition of failure [9&10].

To study the behavior of concrete under the effect of projectile impact, many experiments should be conducted, which are relatively expensive. A Nonlinear three-dimensional hydro-code numerical simulation was carried out using AUTODYN 3D [11], which is an extensive software dealing with complex interaction of projectile with concrete. In the simulation, steel ogive-nose projectile with a diameter of 23 mm is fired against concrete panels with striking velocity 980 m/s. Fourteen numerical tests were carried out to study the reinforcement parameters that affect the penetration resistance of wire mesh reinforced concrete panels. The parameters included are the reinforcement ratio; reinforcement position; and reinforcement distribution.

2. Numerical Simulation Planning and Objectives

A preliminary design of the reinforced concrete panels is carried out to identify the strength and concrete dimensions as well as the proper reinforcement ratio. The design procedure is made using the already existing empirical formulae developed for penetration resistance [12]. The wire steel mesh reinforced concrete panel dimensions are set to (550 ×550 ×300 mm) to account for steel blunt-nose projectile type, 23 mm in diameter and a mass of 175 grams. Fourteen numerical simulation tests were planned for varying reinforcement ratio and placement for different concrete panels as listed in Table 1. The main objectives include the study of:

- The effect of reinforcement ratio on the penetration resistance.
- The influence of wire steel meshes position and distribution along the panel thickness.

In order to achieve these objectives, the numerical simulations are planned as follows:-

1. Numerical simulations named (T1R–T6R) were performed to study the influence of reinforcement ratio on the penetration resistance of concrete panels. The wire steel meshes are placed in the rear face of the panels.
2. Two reinforcement ratios are selected from the results obtained in the previous step (1.5% and 3%) to be used in investigating the influence of reinforcement position and distribution on penetration resistance. The wire steel meshes reinforcement that satisfy the reinforcement ratio (T4R: 1.5%) is employed through three numerical simulations (T4W, T4RH & T4FH). In which (T4W) the meshes are distributed equally spaced through the whole thickness of the panel. In (T4RH), the same number of wire meshes are distributed equally spaced through the rear half of the thickness of the panel, while in (T4FH), it is distributed equally spaced through the front half of the thickness of the panel.

3. The parametric studies carried out in steps (2) are then repeated for reinforcement ratio (T6R: 3%). The wire steel meshes reinforcement that satisfy the reinforcement ratio (T6R: 3%) is employed through three numerical simulations (T6W, T6RH & T6FH). In which (T6W) the meshes are distributed equally spaced through the whole thickness of the panel. In (T6RH), the same number of wire meshes

are distributed equally spaced through the rear half of the thickness of the panel, while in (T6FH), it is distributed equally spaced through the front half of the thickness of the panel.

3. Finite Element Model.

The AUTODYN-3D software package was used in developing the finite element model proposed to simulate the penetration process of projectiles into different concrete panels. The concrete panels and the projectile are modelled as Lagrangian meshes in all models, while the reinforcing wire steel meshes were modelled as beam elements. The geometry and meshes of the projectile, concrete panels and wire steel meshes are described below. The material models depend on the physical material's properties. Table 2 illustrates the basic information specified for each material. Typically four basic types of information are specified for each material [11].

3.1 Projectile

The geometry of the projectile part was defined in all models using unstructured Lagrangian mesh with Four-node quadrilateral elements. Due to the symmetric conditions, the projectile geometry, which is 23 mm diameter and 64 mm length is modelled as a half cylinder, it is divided to 704 elements. The main material parameter for steel used in projectile was chosen from the AUTODYN material library (STEEL 4340) and modified according to the values obtained from material data sheet and listed in Table3. Fig. 1(a) shows the geometry and mesh description for the projectile part.

3.2 Target reinforced concrete panels

The wire steel mesh reinforced concrete target is defined using unstructured Lagrangian mesh with four-node quadrilateral elements. Due to the symmetric conditions, the geometry of each panel (square 550 mm side length and 300 mm thickness) was modeled as half box. It was divided into 243000 elements. Zoning technique was used to refine the meshes in critical region; the element size was 2 X 2 X 5 mm in the impact (maximum stress) region. The material model for concrete was chosen from the AUTODYN material library as (Concrete 35 MPa) and modified according to the values listed in Table 4 [11]. Fig. 1(b) shows the geometry and meshing of the concrete panel.

The dimension of expanded wire steel meshes used in simulations is (550 x 550 mm). In case of using wire meshes of 3 mm thickness, the size of the opening is (16 x 38 mm) and in case of wire steel meshes of 5 mm thickness the opening size is (30 x 90 mm). The material model used to represent the wire steel mesh is Johnson Cook strength model with material type chosen from the AUTODYN library (STEEL 1006) and modified as listed in Table 5 [11]. Fig. 2 illustrate sample of the wire meshes used for simulation (T6W).

3.3 Initial and boundary conditions

The initial condition for projectile velocity used in numerical simulation in all analytical tests is equal to 980 m/sec, directed in the negative Z direction as shown in Fig. 3(a).

The boundary conditions of the nodes located on the rear face of the concrete panels are defined as constant velocity in Z direction (Vz = 0). While the boundary conditions of the nodes located on the lower face of the concrete panels are defined as constant velocity in Y direction (Vy=0), Fig. 3(b) illustrate the boundary conditions on the concrete panel surface.

4. Interaction Model.

Two types of interaction may be defined in AUTODYN-3D [11]: Lagrange/Lagrange and Euler/ Lagrange interaction. In current numerical simulation, impact slide surface was between two Lagrange subgrids, so the interaction between these sub-grids is specified as Lagrange/Lagrange interaction. Projectile – concrete interaction was achieved using the TRAJECTORY interaction logic. The Trajectory contact algorithm is implemented for all unstructured Lagrangian solvers.

5. Results and Discussion

The results of the fourteen numerical simulation tests are listed in Tables 6 & 7 and discussed here after. The relative comparisons of the output of these parametric studies are based on three measured main indices that are reversely proportional to the penetration resistance: the penetration depth, the front face damaged area and the rear face damaged area. A list of figures: Fig.4 to Fig.10 represent samples of the simulation results that are used to illustrate the penetration – time history, penetration depth and developed stresses at front face due to projectile penetration.

5.1 Effect of reinforcement ratio

Based on the literature review, there is a dispute over the optimal value and position of the reinforcement for concrete panels subjected to projectile impact. Accordingly, many values of reinforcement ratio were considered in the numerical simulations as it has increased sequentially from (T1R: 0.37%) to (T6R: 3%) as listed in Table 1. The wire steel meshes placed

in the tension side at the rear face of the panels with respect to the projectile direction. The results of simulations (T1R to T6R) are listed in Table 6, from which it can be seen that the reinforcement ratio has insignificant influence on the penetration resistance. This finding can be attributed to the position of the reinforcement as it is concentrated at the rear face. The penetration interaction of the projectile starts at the front face, dissipating most of its kinetic energy through the whole panel depth till it reaches the reinforcement at rear face. Consequently, based on such an interaction sequence, the compressive strength of concrete panel is considered as the only parameter that can influence the penetration resistance.

5.2 Effect of reinforcement position and distribution

Based on the simulation results (T1R to T6R), the simulations (T4F:1.5%) and (T6F:3%) were carried out, in which the reinforcement concentrated at the front face for comparison with its counterparts (T4R:1.5%) and (T6R:3%) respectively. The results are listed in Table 7 from which it can be seen that the change of the reinforcement position, from rear to front face, decreased the penetration depth by approximately 15 % for both reinforcement ratios. From Fig.(5 to 8) labelled (a) show the penetration of the projectile through the thickness and Fig.(5 to 8) labelled (b) show the Von Misses stress distribution on the face of the panel. These figures prove that the stresses concentration decreased in (T4F& T6F) compared with their counterparts ((T4F& T6F) respectively leading to decrease in the damaged area. This can be attributed to the increase of the tensile strength at the front face caused by the existence of the wire steel meshes at the front. Also, the latest simulations results confirmed that the reinforcement ratio has no influence on the penetration resistance; however, the position of reinforcement has direct influence on penetration resistance.

In sight of the aforementioned simulation results, it was crucial to consider the reinforcement distribution along the thickness of concrete panel as an important parameter that may influence the penetration resistance. Accordingly, four simulation tests were carried out in which two reinforcement ratios (1.5% and 3%) were employed to examine the influence of this parameter. In simulation test (T4RH, T4FH and T4W), the wire steel meshes of reinforcement ratio 1.5% were distributed equally spaced along the rear half, the front half and the whole depth respectively. Also, in simulation test (T6RH, T6FH and T6W), the wire steel meshes that represent reinforcement ratio 3% is distributed equally spaced along the rear half, the front half and the whole depth respectively. Table 7 summarizes the results of simulation (T4RH, T4FH and T4W) compared to its counterpart (T4R) and the results of simulation (T6RH, T6FH and T6W) compared to its counterpart (T6R). The results lead to the following findings:

- The distribution of the reinforcement along the rear half (T4RH and T6RH) have a slight influence on the penetration resistance compared to its counterparts (T4R and T6R) respectively.
- The distribution of the reinforcement along the whole thickness represented by simulation (T4W and T6W) compared to the same references, have better performance in penetration resistance by 8.5% and 12% respectively.
- In simulations (T4FH and T6FH), the distribution of steel wire meshes in the front half enhanced the penetration resistance by 11.4% and 14.1% respectively. However, the concentration of the steel wire meshes at front face in (T4F and T6F) proved to improve the penetration resistance by relatively higher values 14.5% and 15.9% respectively.

Conclusions

The previous results discussion leads to the following conclusions:

- Increasing the reinforcement ratio has insignificant influence on penetration resistance whether it is placed at the rear or front face.
- The position of the wire steel meshes in the concrete panel has a relatively positive influence on the penetration resistance as the penetration depth improved by 15% when it is concentrated at the front face instead of the rear face. Such result can be attributed to the existence of the full reinforcement at the front face (full capacity of panel tensile strength) causing a remarkable dissipation of the projectile kinetic energy at its highest value and at early timing in the penetration process.
- The distribution of the wire steel meshes along the front half relatively improved the penetration resistance compared to those distributed along the whole thickness or concentrated at the rear face of concrete panel.
- The size of damage at front and rear areas is reduced with the increase of reinforcement ratio.

References

[1] Gold, V.M., "Analysis of the penetration resistance of concrete" U.U. Army Armament Research, 1997.
[2] Jason T. and Gomeza, A.S., "Multiple impact penetration of semi-infinite concrete". International Journal of Impact Engineering, 2001. 25: p. 965–979.
[3] Forrestal MJ, L.V., "Penetration into soil targets", International Journal of Impact Engineering, 1992. 12: p. 427-44.
[4] J. Buchar, J.V., S. Rolc and M. Lazar, "Response of concrete to the impact of fragments simulating projectiles", 20th International Symposium on Ballistics, ORLANDO, 2002.
[5] Avraham N. and Dancygier, D.Z.Y., Chanoch Jaegermann, "Response of high performance concrete plates to impact of non-deforming projectiles", International Journal of Impact Engineering, 2007. 34: p. 1768–1779.
[6] Murtiadi, S., "Behavior of high strength concrete plates under impact loading", M.Sc. thesis, faculty of engineering and applied science, memorial university of new found land, Canada, 1999.
[7] Yankelevsky, et. al., "High strength concrete response to hard projectile impact", International Journal of Impact Engineering, 1996. 18(6): p. 583-599.
[8] ACI committee 549, "State-of-the-Art Report on Ferrocement", American Concrete Institute, Technical Report no. 549R-97, 1997.
[9] Zhang M. H., L.L., and Paramasivam P., "Flexural toughness and impact resistance of steel-fibre-reinforced lightweight concrete". Magazine of Concrete Research, 2004. 56(5): p. 251-262.
[10] Abdullah, K.T., Koshiro N., and Shingo H., "Behavior of Ferrocement Subjected to Missile Impact", Transactions of the 17th International Conference on Structural Mechanics in Reactor Technology, Prague, Czech Republic, 2003.
[11] Dynamics, A.E.S.f.N.-l., AUTODYN Electronic Document Library. Multiversions, Century Dynamics Inc., 2005.
[12] X.W. Chena, X.L.L., F.L. Huang, H.J. Wu, Y.Z. Chen, "Normal perforation of reinforced concrete target by rigid projectile". International Journal of Impact Engineering, 2008. 35: p. 1119-1129.

Table 1: Details of Numerical Simulation

No.	Test	Meshes Number & Size (mm)	Reinforcement Ratio	Reinforcement Position
1	T1R	1 mesh ϕ 3mm	0.37%	Concentrated in the Rear face
2	T2R	1 mesh ϕ 5mm	0.56%	Concentrated in the Rear face
3	T3R	2 mesh ϕ 5mm	0.75%	Concentrated in the Rear face
4	T4R	4 mesh ϕ 5mm	1.5%	Concentrated in the Rear face
5	T5R	6 mesh ϕ 5mm	2.25%	Concentrated in the Rear face
6	T6R	8 mesh ϕ 5mm	3%	Concentrated in the Rear face
7	T4F	4 mesh ϕ 5mm	1.5%	Concentrated in the Front face
8	T4RH	4 mesh ϕ 5mm	1.5%	Equally distributed in the Rear half of the specimen
9	T4FH	4 mesh ϕ 5mm	1.5%	Equally distributed in the Front half of the specimen
10	T4W	4 mesh ϕ 5mm	1.5%	Equally distributed in the Whole specimen
11	T6F	8 mesh ϕ 5mm	3%	Concentrated in the Front face
12	T6RH	8 mesh ϕ 5mm	3%	Equally distributed in Rear half of the specimen
13	T6FH	8 mesh ϕ 5mm	3%	Equally distributed in Front half of the specimen
14	T6W	8 mesh ϕ 5mm	3%	Equally distributed in the Whole specimen

Table 2: Basic Information Specified for each Material.

	Projectile	Concrete Panels	Reinforcing Steel
Equation of State	Linear	P-Alpha	Linear equation
Strength model	Johnson Cook	RHT	Piecewise JC
Failure model	Johnson Cook	RHT	None
Erosion model	Instantaneous geometrical	Instantaneous geometrical	Instantaneous geometrical

Table 3: Mechanical Properties of the 23 AP Projectile Materials.

Brinell hardness number (HB)	Yield strength (MPa)	Ultimate strength(MPa)	Strain to fracture (%)
475	1726	1900	7

Table 4: Mechanical Properties of Concrete.

Property	Density(kg/m3)	Compressive strength (MPa)	Tensile strength(MPa)	Modulus of elasticity (GPa)
value	2360	70	3.1	29

Table 5: Mechanical Properties of Steel Mesh.

Property	Density(kg/m3)	Yield strength (MPa)	Ultimate strength(MPa)	Modulus of elasticity (GPa)
value	7850	250	460	210

Table 6: Results of Numerical Simulation for Reinforcement Concentrated at Rear or Front face.

No.	Model	Reinforcement Ratio	Penetration Depth (cm)
1	T1R	0.37%	23
2	T2R	0.56%	22.6
3	T3R	0.75%	22.5
4	T4R	1.5%	22.4
5	T5R	2.25%	22.2
6	T6R	3%	22
7	T4F	1.5%	19.15
8	T6F	3 %	18.5

Table 7: Results of Numerical Simulation for Reinforcement Distributed Through the Panel Thickness.

No.	Test	Reinforcement Position	Penetration Depth (cm)	% Decrease in Penetration Depth
1	T4R	Concentrated in the Rear face	22.4	---
2	T4RH	Equally distributed in the Rear half	21.2	5.4%
3	T4F	Concentrated in the Front face	19.15	14.5%
4	T4FH	Equally distributed in the Front half	19.84	11.4%
5	T4W	Equally distributed in the whole thickness	20.5	8.5%
6	T6R	Rear face	22	---
7	T6RH	Equally distributed in the Rear half	21	4.55%
8	T6F	Concentrated in the Front face	18.5	15.9%
9	T6FH	Equally distributed in the Front half	18.9	14.1%
10	T6W	Equally distributed in the whole thickness	19.35	12%

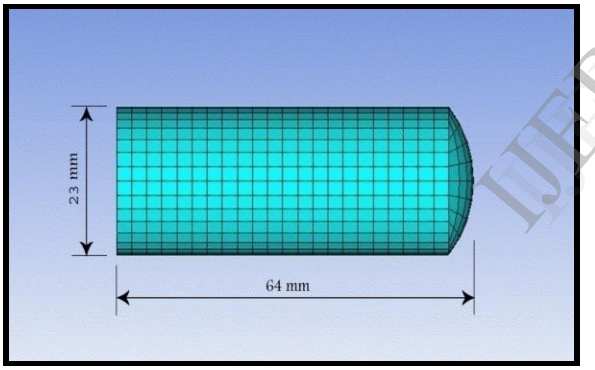

Fig. 1(a): Dimensions and meshing of the projectile.

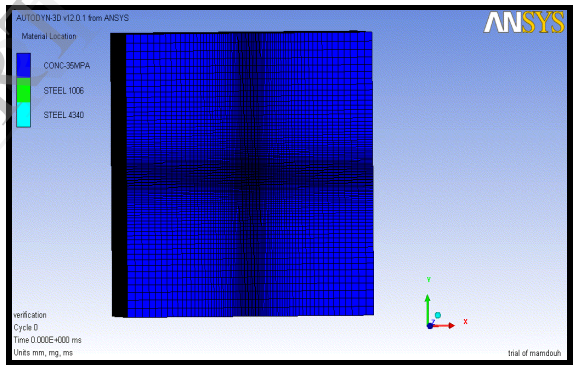

Fig. 1(b): Geometry and meshing of concrete panels.

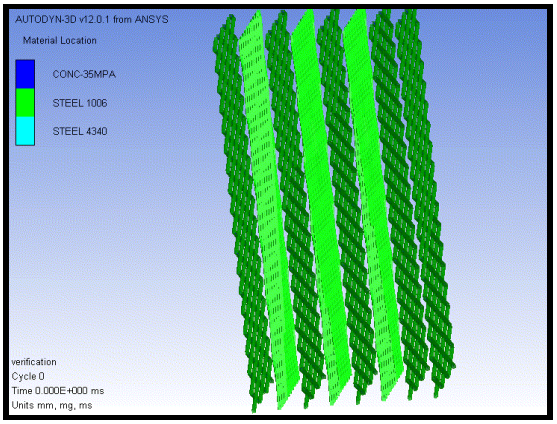

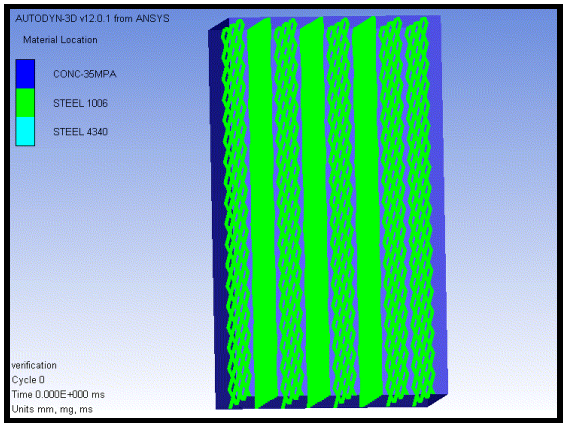

Fig. 2: Steel layers distribution in (T6W).

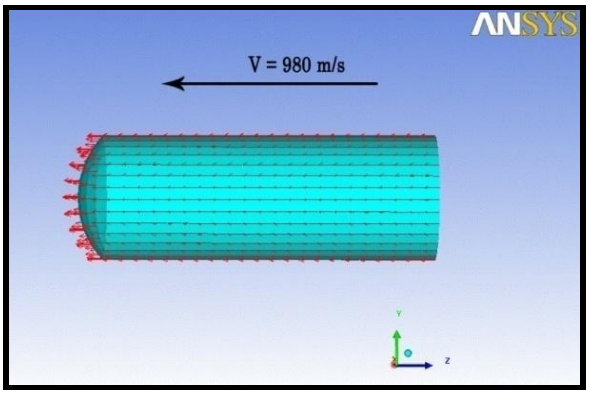

Fig. 3(a): Initial condition of projectile.

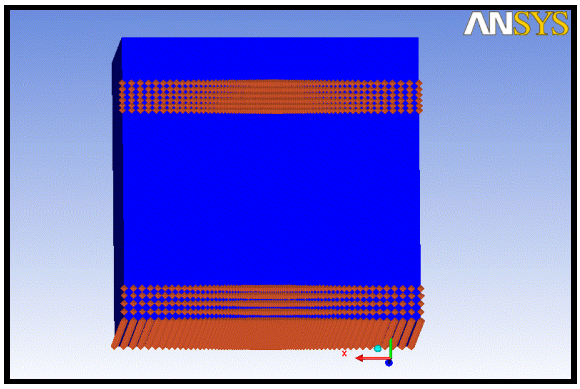

Fig. 3(b): Boundary conditions of targeted concrete panel.

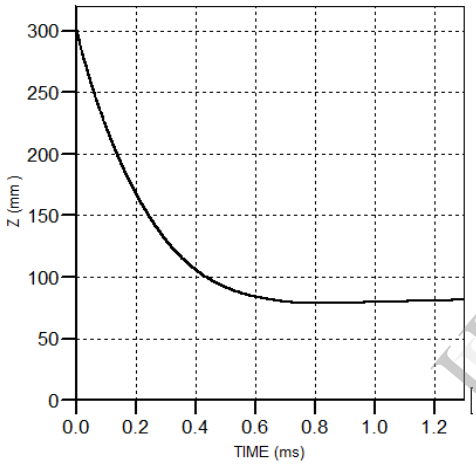

Fig. 4(a): Penetration-time history for test (T4R).

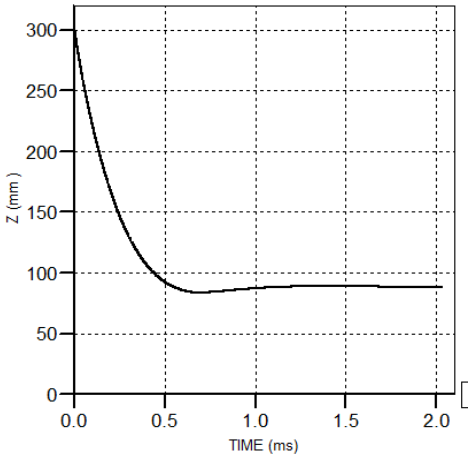

Fig. 4(b): Penetration-time history for test (T4RH).

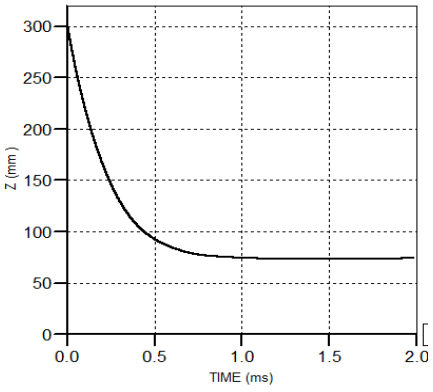

Fig. 4(c): Penetration-time history for test (T6R).

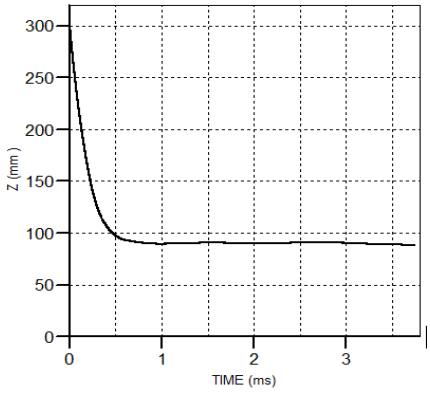

Fig. 4(d): Penetration-time history for test (T6RH).

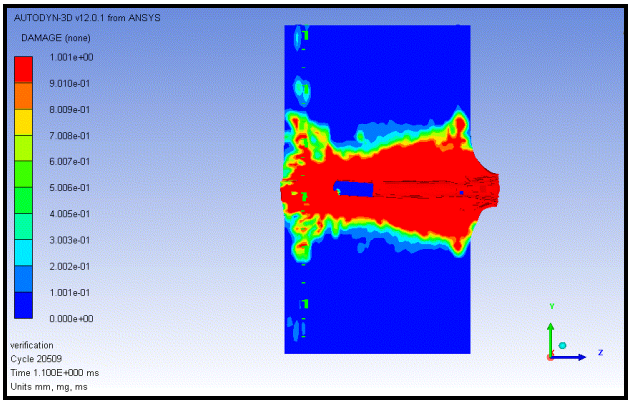

Fig. 5 (a): Penetration depth for test (T4R).

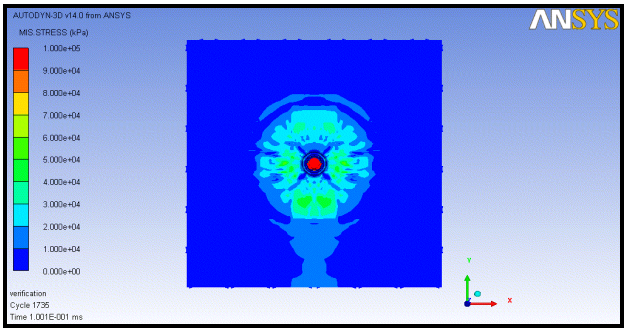

Fig. 5 (b): Stress distribution at front face for test (T4R).

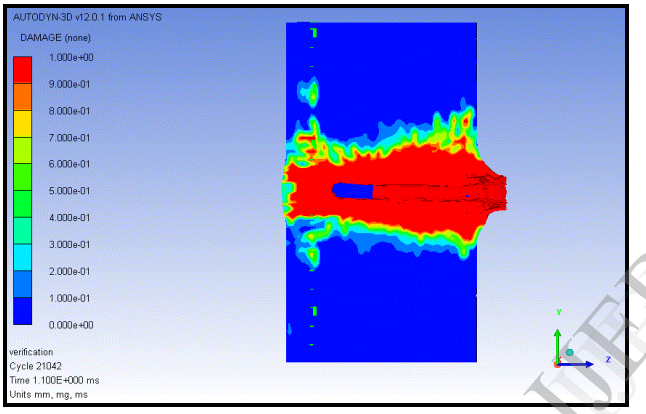

Fig. 6 (a): Penetration depth for test (T6R).

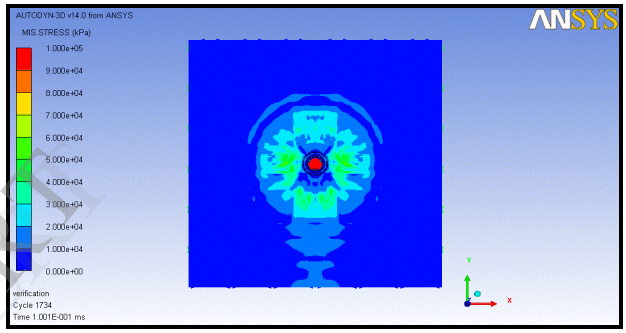

Fig. 6 (b): Stress distribution at front face for test (T6R).

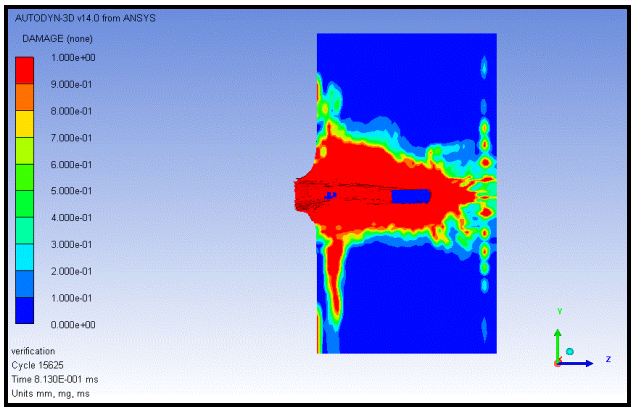

Fig. 7 (a): Penetration depth for test (T4F).

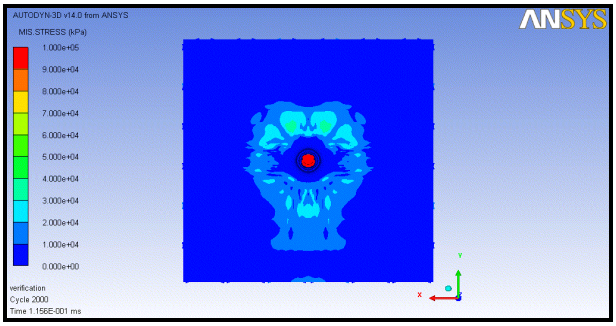

Fig. 7 (b): Stress distribution at front face for test (T4F).

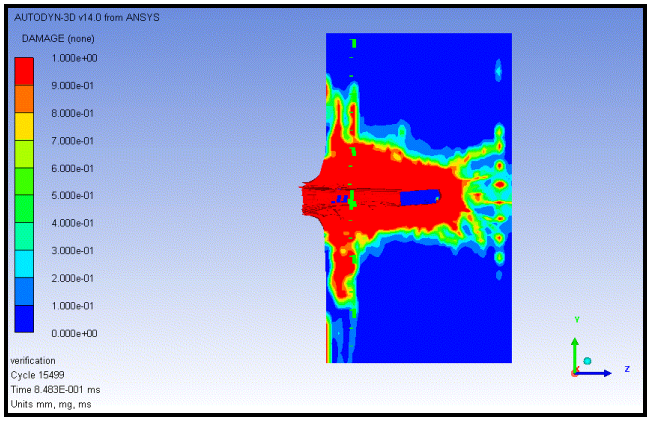

Fig. 8 (a): Penetration depth for test (T6F).

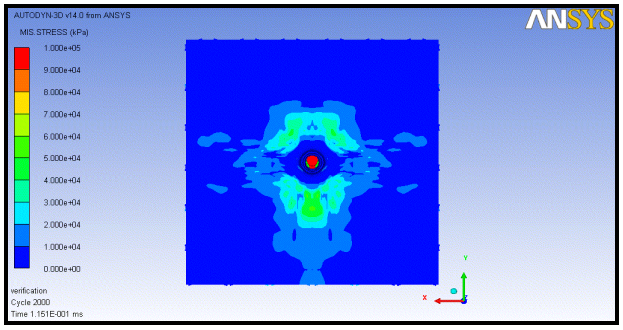

Fig. 8 (b): Stress distribution at front face for test (T6F).

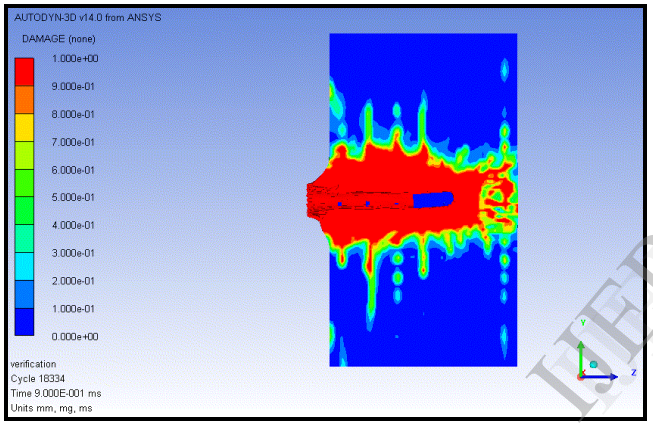

Fig. 9 (a): Penetration depth for test (T4FH).

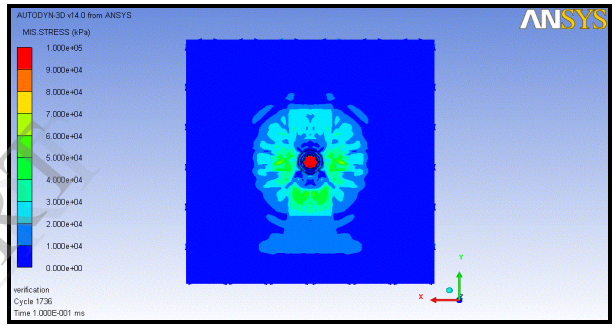

Fig. 9 (b): Stress distribution at front face for test (T4FH).

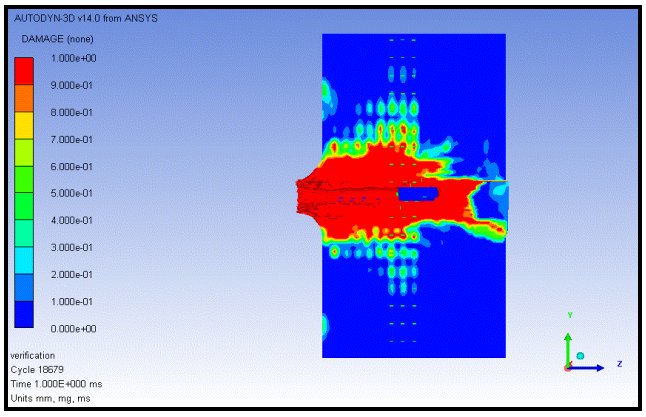

Fig. 10 (a): Penetration depth for test (T6FH).

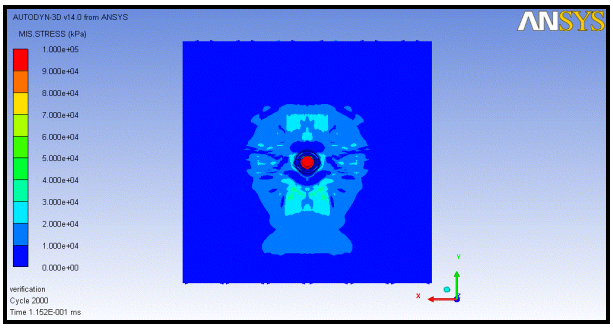

Fig. 10 (b): Stress distribution at front face for test (T6FH).